

# Synthesis and Investigation of Nematic Liquid Crystals with Flexoelectric Properties

Janine H. Wild,<sup>†</sup> Kevin Bartle,<sup>‡</sup> Nicola T. Kirkman,<sup>‡</sup> Stephen M. Kelly,<sup>\*,†</sup> Mary O'Neill,<sup>\*,‡</sup> Tom Stirner,<sup>‡</sup> and Rachel P. Tuffin<sup>\*,§</sup>

Departments of Physics and Chemistry, University of Hull, Cottingham Road, Hull, HU6 7RX, U.K., and Qinetiq, Malvern, Worcestershire, WR14 3PS, U.K.

Received July 29, 2005. Revised Manuscript Received September 23, 2005

We describe the synthesis and characterization of a series of model nematic liquid crystals with transverse dipole moments used to study the flexoelectric effect in guest–host mixtures with commercial liquid crystal host. The flexoelectric coefficient of the mixtures, containing only 10% by weight of the dopant, are up to 6 times higher than those of the pure hosts. The length, bend angle, and dipole moments of the molecules are systematically varied to investigate any correlations with the flexoelectric effect. We find that the flexoelectric coefficients increase with molecular length, are inversely correlated with the bend angle, and are independent of the dipole moment of the dopant. Although these findings seem to contradict predictions from dipolar flexoelectric theories, they can be reconciled by considering the properties of both the guest and host in the mixture. Thiophenes and dimesogens show particularly large flexoelectric effects. This work should inform the molecular design of new materials with enhanced flexoelectric properties.

## I. Introduction

The flexoelectric effect in the nematic phase is a relatively unexplored but fundamental property of liquid crystals. It originates from a spontaneous polarization induced by splay or bend deformations of the nematic director.<sup>1</sup> The flexoelectric coefficients associated with the splay and bend deformations are defined as  $e_{11}$  and  $e_{33}$ , respectively, in analogy with the corresponding elastic constants,  $k_{11}$  and  $k_{33}$ . The resultant flexoelectric polarization,

$$\mathbf{P} = e_{11}\mathbf{n}(\nabla \cdot \mathbf{n}) + e_{33}\mathbf{n} \times (\nabla \times \mathbf{n}) \quad (1)$$

where  $\mathbf{n}$  is the director, has both the splay and bend contributions adding in the same direction and follows the sign convention of Rudquist and Lagerwall.<sup>2</sup> It has been postulated that an electric field can couple to the gradients in the field director in nematic liquid crystals, if they exhibit strong shape polarity, e.g., they are banana-, pear-drop-, or wedge-shaped. Figure 1 describes the effect for a banana-shaped molecule. A curvature strain, for example, a bend deformation, gives a preferred molecular orientation and induces a spontaneous polarization because of the associated molecular dipole.<sup>1</sup> However, a rodlike or cigar-shaped molecule can also exhibit flexoelectric properties, but by a quadrupolar, rather than a dipolar, flexoelectric effect.<sup>3</sup>

The flexoelectric effect is of general scientific interest as it is a linear effect with the applied electric field, which is

an unusual phenomenon for nematic liquid crystals. The most important application to date is to switch bistable liquid crystal displays (LCDs). A range of sub-millisecond LCDs based on the flexoelectric effect in chiral nematic<sup>4–6</sup> and nematic liquid crystals<sup>7–9</sup> are in the process of being developed. LCDs based on flexoelectric nematic liquid crystals have the potential to satisfy the future requirements over the medium term of the flat panel displays industry in terms of performance, manufacturability, and cost. However, one of the major constraints to the development of bistable nematic displays is the absence of liquid crystal mixtures specifically designed and optimized for the flexoelectric effect. Some bistable nematic prototypes<sup>6,9</sup> incorporate the homologues of the nematic liquid crystal 4-cyano-4'-pentyl-biphenyl (K15) first synthesized almost 30 years ago. Dimesogenic liquid crystals (symmetrical dimers) have been reported for chiral nematic LCDs using the flexoelectric effect.<sup>10</sup> A banana-shaped molecular dopant was found to increase by 40% the flexoelectric effect in the commercial nematic mixture E7 from E. Merck.<sup>11</sup> The nematic phase of a short liquid crystal with a rodlike shape was reported to

- (4) Patel, J. S.; Meyer, R. B. *Phys. Rev. Lett.* **1987**, *58*, 1538.
- (5) Rudquist, P.; Komitov, L.; Lagerwall, S. T. *Phys. Rev. E* **1994**, *50*, 4735.
- (6) Coles, H. J.; Musgrave, B.; Coles, M. J.; Willmott, J. *J. Mater. Chem.* **2001**, *11*, 2709.
- (7) Barberi, R.; Giocondo, M.; Durand, G. *Appl. Phys. Lett.* **1992**, *60*, 1085.
- (8) Bryan-Brown, G. P.; Towler, M. J.; Bancroft, M. S.; McDonnell, D. G. *Proceedings IDRC '94*, Monterey, 1994; p 209. Bryan-Brown, G. P.; Brown, C. V.; Jones, C. J.; Wood, E. L.; Sage, I. C.; Brett, P.; Rudin, J. *Proceedings SID 97 Digest*, Boston, 1997; p 37.
- (9) Dozov, I.; Nobili, M.; Durand, G. *Appl. Phys. Lett.* **1997**, *70*, 1179.
- (10) Musgrave, B.; Lehman, P.; Coles, H. J. *Liq. Cryst.* **1999**, *28*, 1235.
- (11) Hermann, D. S.; Komitov, L.; Lagerwall, S. T.; Heppke, G.; Rauch, S. *Proceedings of the 27th Freiburg Liquid Crystal Conference*, 1998; p 57.

\* Authors to whom correspondence should be addressed. E-mail: s.m.kelly@hull.ac.uk. E-mail: m.oneill@hull.ac.uk.

<sup>†</sup> Department of Physics, University of Hull.

<sup>‡</sup> Department of Chemistry, University of Hull.

<sup>§</sup> Qinetiq.

(1) Meyer, R. B. *Phys. Rev. Lett.* **1969**, *22*, 918.

(2) Rudquist, P.; Lagerwall, S. T. *Liq. Cryst.* **1997**, *23*, 503.

(3) Prost, J.; Marcerou, J. P. *J. Phys.* **1977**, *38*, 315.

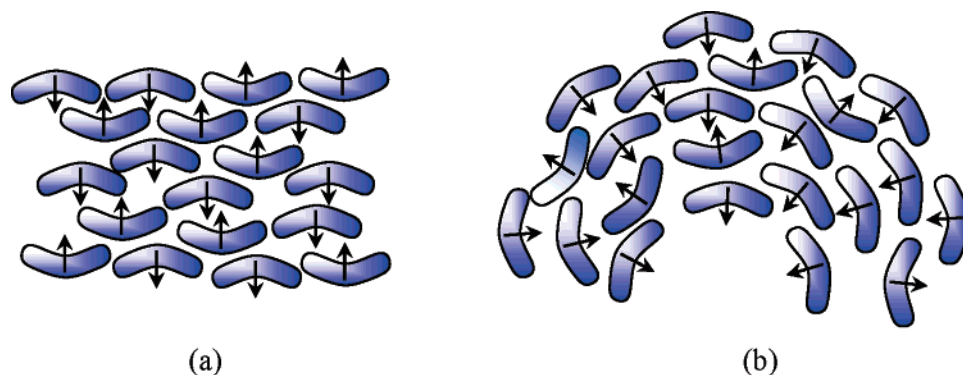


**Figure 1.** (a) Unstrained configuration for a nematic liquid crystal with polar banana-shaped molecules. (b) Bend deformations coupled to a nonzero polarization.

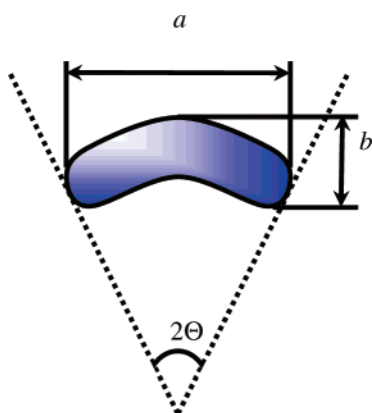


**Figure 2.** Geometrical model used by Helfrich to quantify the length  $a$ , breadth  $b$ , and bend angle  $\Theta$  of the banana shape.<sup>13</sup>

exhibit relatively large flexoelectric coefficients in the pure state at room temperature.<sup>12</sup> There are also a number of theories and models which attempt to correlate molecular structure to the flexoelectric effect.<sup>3,13–18</sup> However, they all place a different emphasis on the importance of shape anisotropy as well as dipolar and quadrupolar effects and require verification. For example, Helfrich uses Meyer's dipolar model to establish theoretical expressions for the flexoelectric coefficients. He found that  $e_{33} \propto \Theta(b/a)^{2/3}\mu$  for a banana-shaped molecule, where the molecular parameters, length  $a$ , breadth  $b$ , and bend angle  $\Theta$  are defined in Figure 2 and  $\mu$  is the transverse dipole moment.<sup>13</sup> Osipov found that dipolar effects are only significant in banana-shaped molecules with a transverse dipole moment and agrees that  $e_{33} \propto \Theta\mu$  but argues that it is also proportional to  $a$ .<sup>15</sup> Therefore, an understanding of the relationship between molecular structure of nematic liquid crystals and the flexoelectric coefficients would be both scientifically interesting and potentially of significant commercial interest. We now report the results of our attempt to carry out such a study. We study the flexoelectric effect in novel banana-

shaped liquid crystals used as dopants in commercial nematic liquid crystals. The flexoelectric coefficients are measured as  $e/k = (e_{11} + e_{33})/k$ , where  $k$  is the elastic constant using the one constant approximation. Two main classes of liquid crystal dopants are studied, three-ringed heterocyclics<sup>19</sup> and dimesogens. These compounds have  $C_{2v}$  symmetry and have no longitudinal dipole moment. We systematically change the shape and transverse dipole moment of the dopants and study the resulting changes in the flexoelectric effect of the mixtures. Very large variations are found: a dopant concentration of only 10 wt % can increase the flexoelectric effect of the host by a factor of 6–7. Although the data has significant scatter, two general trends are clearly identified. The flexoelectric effect is relatively insensitive to the magnitude of the dipole moment of the dopant but is correlated with molecular length and bend angle.

## II. Experimental Section

**Materials Synthesis.** The 2,6-bis(4-pentylphenyl)pyridazine **1** was produced according to a literature procedure by ring closure in glacial acetic acid under reflux in the presence of hydrazine monohydrate of the diketone produced by the Friedel–Crafts reaction of pentylbenzene with fumaryl chloride.<sup>20</sup> The difluoro-terphenyl **2** (Cr-N = 45 °C; N-I = 116 °C) was supplied by E. Merck (Dr. D. Coates). The heterocycles **3** and **4** were synthesized according to a modified literature procedure by ring closure reactions of *N,N'*-bis(4-pentyl-1-carbonylphenyl)hydrazine, which was produced from the corresponding hydrazone prepared by reacting **2** equiv of the acid chloride of 4-pentylbenzoic acid with hydrazine monohydrate. The 2,5-disubstituted-1,3,4-oxadiazole **4** was produced by a ring closure using phosphoryl chloride, whereas 2,5-disubstituted-1,3,4-thiadiazole **3** was prepared using phosphorus-(penta)sulfide and pyridine.<sup>21</sup> The methods of synthesis of the thiophenes **5–8** and the dimers **9–13** have been reported elsewhere.<sup>12,22</sup> The structures of intermediates and final products were confirmed by proton (<sup>1</sup>H) nuclear magnetic resonance (NMR) spectroscopy (JEOL JMN-GX270 FT nuclear resonance spectrometer), infrared (IR) spectroscopy (Perkin-Elmer 783 infrared spec-

(12) Campbell, N. L.; Duffy, W. L.; Thomas, G. I.; Wild, J. H.; Kelly, S. M.; Bartle, K.; O'Neill, M.; Minter, V.; Tuffin, R. P. *J. Mater. Chem.* **2002**, *12*, 2706.

(13) Helfrich, W. Z. *Naturforsch.* **1971**, *26a*, 833.

(14) Ponti, S.; Zihlerl, P.; Ferrero, C.; Zumer, S. *Liq. Cryst.* **1999**, *26*, 1171.

(15) Osipov, M. A. *Sov. Phys. JETP* **1983**, *58*, 1167.

(16) Singh, Y.; Singh, U. P. *Phys. Rev. A* **1989**, *39*, 4254.

(17) Brown, C. V.; Mottram, N. J. *Phys. Rev. E* **2003**, *68*, 31702.

(18) Ferrarini, A. *Phys. Rev. E* **2001**, *64*, 021710.

(19) Kishikawa, K.; Harris, M. C.; Swager, T. *Chem. Mater.* **1999**, *11*, 867.

(20) Weygand, C.; Lanzendorf, W. *J. Prakt. Chem.* **1938**, *151*, 221.

(21) Dimitrowa, K.; Hauschild, J.; Zschke, H.; Schubert, H. *J. Prakt. Chem.* **1980**, *322*, 933.

(22) Chapman, J.; Ellis, C.; Duffy, W. L.; Friedman, M. R.; Kelly, S. M.; Thomas, G. I.; Xu, H.; Davey, A. B.; Crossland, W. A. *Mol. Cryst. Liq. Cryst.* **2004**, *411*, 49.

trophotometer), and mass spectrometry (MS) (Finnegan MAT 1020 automated GC/MS). Reaction progress and product purity were checked using a CHROMPACK CP 9001 capillary gas chromatograph fitted with a 10 m CP-SIL 5CB (0.12  $\mu\text{m}$ , 0.25 mm) capillary column. All of the final products were more than 99.5% pure by GLC. Transition temperatures were determined using an Olympus BH-2 polarizing light microscope together with a Mettler FP52 heating stage and a Mettler FP5 temperature control unit. The analysis of transition temperatures and enthalpies was carried out by a Perkin-Elmer DSC7-PC differential scanning calorimeter.

*C,C'-Bis(4-pentyl-1-carbonylphenyl)ethene*. Fumaryl chloride (95) (1.00 g,  $65.0 \times 10^{-4}$  mol) and aluminum chloride (1.76 g,  $130.6 \times 10^{-4}$  mol) were mixed together in DCM (50  $\text{cm}^3$ ) for 30 min. The soluble complex was decanted off and heated to 100  $^\circ\text{C}$  where pentylbenzene (94) (1.94 g,  $130.0 \times 10^{-4}$  mol) was added dropwise to the solution and the solution stirred for 8 h. The cooled mixture was added to dilute hydrochloric acid (50  $\text{cm}^3$ ) and the crude product extracted into diethyl ether (2  $\times$  50  $\text{cm}^3$ ) and dried ( $\text{MgSO}_4$ ). Purification was performed by column chromatography using a 1:1 DCM:hexane mixture to yield the desired diketone (0.89 g, 36%) mp 97.1–97.3  $^\circ\text{C}$ . MS  $m/z$ : 376 ( $\text{M}^+$ ), 175 (100%), 131, 91. IR (KBr)  $\nu_{\text{max}}/\text{cm}^{-1}$ : 2930, 2860, 1646, 1605, 1303, 1189, 852, 736.  $^1\text{H}$  NMR (400): 7.99 (6H, m), 7.32 (4H, d), 2.68 (4H, t), 1.65 (4H, quint), 1.34 (8H, m), 0.89 (6H, t).

*2,5-Bis(4-pentylphenyl)pyridazine 1*. A mixture of *C,C'*-bis(4-pentyl-1-carbonylphenyl)ethene (0.50 g,  $13.3 \times 10^{-4}$  mol) and glacial acetic acid (20  $\text{cm}^3$ ) was heated until reflux and then hydrazine monohydrate (0.15 g,  $27.7 \times 10^{-4}$  mol) was added dropwise. The solution was heated under reflux for 16 h. The cooled reaction mixture was quenched with water (50  $\text{cm}^3$ ) and the product extracted into diethyl ether (2  $\times$  50  $\text{cm}^3$ ), DCM (50  $\text{cm}^3$ ), and the combined organic extracts washed with water (100  $\text{cm}^3$ ) and dried ( $\text{MgSO}_4$ ). The crude product was purified by column chromatography using a 1:4 ethyl acetate:hexane mixture as eluent followed by recrystallization from ethanol and the product was dried in vacuo ( $\text{CaCl}_2$ ) to yield the desired pyridazine **1** (0.08 g, 16%). Transition temperatures ( $^\circ\text{C}$ ): Cr 104, SmC 196 I. Literature value Cr 106, SmC 195 I.<sup>20</sup> MS  $m/z$ : 372 ( $\text{M}^+$ ), 147 (100%), 80, 76. IR (KBr)  $\nu_{\text{max}}/\text{cm}^{-1}$ : 2963, 2849, 1467, 1400, 1285, 1188, 803, 761.  $^1\text{H}$  NMR (270): 7.86 (6H, m), 7.22 (4H, d), 2.67 (4H, t), 1.66 (4H, quint), 1.30 (8H, m), 0.89 (6H, t).

*4-Pentylbenzoyl Chloride*. 4-Pentylbenzoic acid (10.00 g,  $520.0 \times 10^{-4}$  mol) and thionyl chloride (30.99 g, 0.26 mol) were heated together under reflux (4 h). Any unreacted thionyl chloride was removed by evaporation and the crude product (9.87 g, 89%) used without further purification.

*N,N'-Bis(4-pentylbenzoyl) Hydrazine*. 4-Pentylbenzoyl chloride (9.87 g,  $457.4 \times 10^{-4}$  mol) was dissolved in tetrahydrofuran (50  $\text{cm}^3$ ) and added dropwise into stirred hydrazine monohydrate (200  $\text{cm}^3$ ) at 0  $^\circ\text{C}$  and left to stir for 1 h. The crude product was extracted into acetone (100  $\text{cm}^3$ ) and dried ( $\text{MgSO}_4$ ). Purification was achieved by recrystallization from ethanol and the product dried in vacuo ( $\text{CaCl}_2$ ) to yield the desired hydrazine (8.97 g, 51%), mp 127.2–127.5  $^\circ\text{C}$ . MS  $m/z$ : 380 ( $\text{M}^+$ ), 310, 175 (100%), 91. IR (KBr)  $\nu_{\text{max}}/\text{cm}^{-1}$ : 3215, 2861, 1373, 1635, 1466, 1288, 853, 743.  $^1\text{H}$  NMR (400): 10.36 (2H, s), 7.82 (4H, d), 7.32 (4H, d), 2.63 (4H, t), 1.59 (4H, quint), 1.30 (8H, m), 0.85 (6H, t).

*2,5-Bis(4-pentylphenyl)thiadiazole 3*. Phosphorus(penta)sulfide (1.50 g,  $52.6 \times 10^{-4}$  mol) was added portionwise to a stirred solution of *N,N'*-di(4-pentylbenzoyl) hydrazine (2.00 g,  $33.7 \times 10^{-4}$  mol) in pyridine (10  $\text{cm}^3$ ); this suspension was then heated to 100  $^\circ\text{C}$  (14 h). Ethanol (10  $\text{cm}^3$ ) was added to the cooled solution and then the entire solution was added to ice-cooled water (200  $\text{cm}^3$ ). The resultant precipitate was filtered off, washed with water (5  $\times$

100  $\text{cm}^3$ ), and dried in vacuo ( $\text{CaCl}_2$ ). The crude product was then purified by column chromatography on silica gel using DCM as eluent followed by recrystallization from ethanol and the product dried in vacuo ( $\text{CaCl}_2$ ) to yield the desired thiadiazole **3** (0.15 g, 8%). Transition temperatures ( $^\circ\text{C}$ ): Cr 90, SmA 122, N 162 I. Literature values Cr 94, SmA 124, N 162 I.<sup>21</sup> MS  $m/z$ : 378 ( $\text{M}^+$ , 100%), 321, 191, 134. IR (KBr)  $\nu_{\text{max}}/\text{cm}^{-1}$ : 2931, 2860, 1609, 1442, 1410, 1084, 853, 777.  $^1\text{H}$  NMR (400): 7.91 (4H, d), 7.30 (4H, d), 2.67, (4H, t), 1.65 (4H, quint), 1.34 (8H, m), 0.90 (6H, t).

*2,5-Bis(4-pentylphenyl)oxadiazole 4*. A mixture of *N,N'*-bis(4-pentylbenzoyl) hydrazine (1.00 g,  $26.3 \times 10^{-4}$  mol) and phosphoryl chloride (30  $\text{cm}^3$ ) was heated under reflux for 4 h. The cooled mixture was quenched with water (100  $\text{cm}^3$ , 0  $^\circ\text{C}$ ) and left to warm to room temperature. The crude product was extracted into a 1:9 diethyl ether:DCM mixture and dried ( $\text{MgSO}_4$ ). Purification was achieved by column chromatography on silica gel using DCM as eluent followed by recrystallization from ethanol and the product dried in vacuo ( $\text{CaCl}_2$ ) to yield the desired oxadiazole **4** (0.30 g, 32%), mp 127.1–127.3  $^\circ\text{C}$ . MS  $m/z$ : 362 ( $\text{M}^+$ , 100%), 249, 175, 58. IR (KBr)  $\nu_{\text{max}}/\text{cm}^{-1}$ : 2931, 2856, 1497, 1113, 1070, 843, 744, 713.  $^1\text{H}$  NMR (400): 8.04 (2H, d), 7.33 (2H, d), 2.68 (4H, t), 1.66 (4H, quint), 1.34 (8H, m), 0.90 (6H, t).

**Experimental Methods.** The mesomorphic behavior of the compounds **1–13** were investigated between crossed polarizers using optical microscopy. The nematic phase (N), the smectic A (SmA), and the smectic C phase (SmC) were the only phases observed for the compounds **1–13**. Typically nematic droplets were observed on slow cooling from the isotropic liquid of those materials **1–3** and **5–13** found to exhibit a nematic phase. The oxadiazole **4** did not exhibit observable mesomorphism. A Schlieren texture was observed for the other compounds **1–3** and **5–13**, with two- and four-point brushes, which is characteristic of a nematic phase. Another Schlieren texture, this time with only four point brushes, was formed on cooling the nematic phase of the compounds **1** and **13** into the smectic C phase. The color of the optical texture also changed at this transition. The optical texture of the smectic A phase observed on cooling the nematic phase of the thiadiazole **3** exhibits the focal conic texture as well as optically extinct areas in the same sample. The simultaneous presence of these two textures is typical of the calamitic smectic A phase or its chiral equivalent. The elliptical and hyperbolic lines of optical discontinuity characteristic of focal conic defects were also observed. The transition temperatures of the compounds **1–13** were confirmed by differential scanning calorimetry (DSC) and good agreement ( $\approx 1$ –2  $^\circ\text{C}$ ) with those values determined by optical microscopy was obtained. These values were measured twice on heating and cooling cycles on the same sample. The values obtained on different samples of the same compounds were reproducible and no thermal degradation was observed. The baseline of the spectra is relatively flat and sharp transition peaks are observed. The transitions observed, i.e., the melting point (Cr–SmA, Cr–SmC, Cr–N, and Cr–I) and the clearing point (N–I) are both first order as usual. A degree of supercooling below the melting point is often observed on the cooling cycle. However, a monotropic liquid crystalline phase could not be observed for the oxadiazole **4**. Mixtures were made of 10 wt % of each of the compounds in the commercial host materials E7 (Merck) and/or ZLI-4792. The liquid crystal transition temperatures of the mixtures were measured using optical microscopy.

The flexoelectric effect was first measured using a standard room-temperature nematic MBBA<sup>23</sup> [*N*-(4-methoxybenzylidene)-4'-butylaniline] only shortly after a theoretical description of the flexoelectric coefficients had been proposed<sup>13</sup> and many different

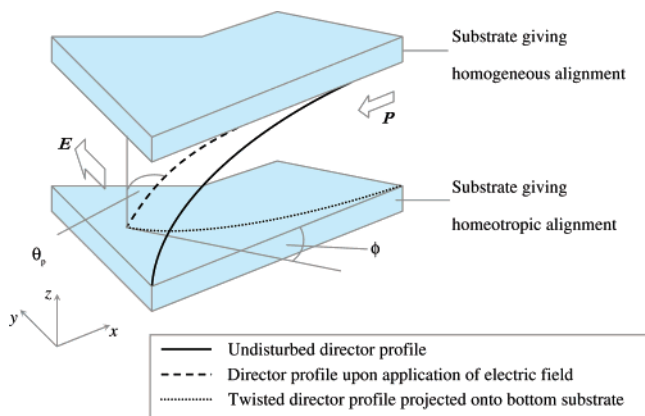


**Figure 3.** Configuration of the hybrid-aligned nematic cell using the flexoelectric coefficients,  $e/k$ .<sup>24</sup>

values for the same compounds, mostly MBBA and K15, have been reported. More reliable methods for measuring the flexoelectric coefficients, especially using the hybrid aligned nematic (HAN) cell, see Figure 3, have been reported recently.<sup>24–29</sup>

We obtain the flexoelectric coefficients,  $e/k$ , from the field-induced twist of a hybrid aligned nematic (HAN) cell of thickness  $d$ .<sup>24</sup> Figure 3 shows the sample geometry of the test cell where a nematic phase is sandwiched between two parallel substrates of glass or plastic. The nematic director is aligned homogeneously at one surface (parallel to the substrate) and homeotropically at the other (perpendicular to the second substrate). This produces a change of  $90^\circ$  in the nematic director profile across the cell with a high degree of splay and bend distortion, which in turn gives rise to a flexoelectric field across the cell.<sup>24,27</sup> A dc electric field,  $E$ , applied perpendicular to the splay-bend deformation, couples to the induced flexoelectric polarization,  $P$ , resulting in a twist of the director in the plane perpendicular to the substrates.  $\theta_p$  is the polar angle. The twist angle at the homeotropic surface,  $\phi$ , can be determined by the measurement of the degree of rotation of incident linearly polarized light. The flexoelectric coefficients are found from the relationship  $e/k = \pi\phi/Ed$ . This method uses an in-plane electric field so that the results are not compromised by surface effects. The test cells were provided by Qinetiq and had an average cell gap of  $50 \mu\text{m}$ . The flexoelectric coefficients collated in the Tables

1–3 are those measured just below the nematic clearing point of the mixture ( $0.98 \times T_{N-1}$  in K) to facilitate comparison at the same reduced temperature. The measurement error is 10% incorporating errors from both the gradient of  $\phi$  versus  $E$  and the cell gap. A semiempirical Hamiltonian (SEH) method, based on the Austin Model 1 function, was used to calculate the dipole moment of each of the molecules.<sup>30</sup> Molecular structures were minimized with respect to their energy using Cerius<sup>2</sup> Smart Minimizer. The molecular length  $a$  and breadth  $b$  were measured using the energy-minimized structures. The bend angle,  $\Theta$ , used in this study is defined, using the small-angle approximation, as  $2(b-w)/a$  where  $w$  is the diameter of an aromatic ring. The molecules have many conformations of equal energy so that care must be taken when distinguishing between the  $\Theta$  values of different compounds.

However, we ensure that  $\Theta$  is a valid parameter by using compounds with relatively short aliphatic end chains and having a very wide range of  $\Theta$  (0.15–0.8 rad).

### III. Experimental Results and Discussion

According to dipolar theory, banana-shaped molecules have no  $e_{11}$  term.<sup>15</sup> However, the flexoelectric effect in the guest–host mixtures may have both splay and bend terms because of the host contribution. Two host materials with different molecular and dielectric properties were chosen. E7 is a cyanobiphenyl mixture with an extremely large dipole moment. The constituent molecules of E7 tend to associate in dimer pairs.<sup>31</sup> It is speculated that antiparallel alignment of the polar end groups may lead to a quadrupolar charge distribution and therefore a significant quadrupolar contribution to the flexoelectric effect.<sup>3,15</sup> The HAN configuration may also induce a shape anisotropy in the dimer. The host mixture ZLI-4792 is also polar but has polyfluorinated, rather than cyano-terminated, nematic liquid crystals, with a lower overall value of the dielectric anisotropy. It does not tend to dimerize. At room temperature the value of  $(e_{11} + e_{33})/k$  was calculated to be  $0.8 \text{ C N}^{-1} \text{ m}^{-1}$ . Using a generalized one constant approximation for  $k$  of 11.6 pN (gained from  $k_{11} = 11.1 \text{ pN}$ ,  $k_{22} = 6.6 \text{ pN}$ , and  $k_{33} = 18.5 \text{ pN}$ ), the value at room temperature gives  $1.3 \pm 0.2 \times 10^{-11} \text{ C m}^{-1}$  for  $(e_{11} + e_{33})$ . This is in reasonable agreement with a literature value of  $(1.5 \pm 0.2) \times 10^{-11} \text{ C m}^{-1}$  for  $(e_{11} + e_{33})$  determined using a fully leaky waveguide mode of study.<sup>29</sup>  $e/k$  is equal to  $0.9 \text{ C N}^{-1} \text{ m}^{-1}$  for E7 at the reduced temperature of  $0.98 T_{N-1}$  and, as expected, the corresponding value for ZLI-4792 is lower and equal to  $0.6 \text{ C N}^{-1} \text{ m}^{-1}$ .

Three different classes of dopants were used to investigate the correlation between the molecular structure of the dopant and the flexoelectric effect in guest–host mixtures. The parameters  $\Theta$ ,  $\mu$ , and  $a$  of the dopants **1–13** and the flexoelectric coefficients of the mixtures are plotted in Tables 1–3. Table 1 shows the data from a series of three ring compounds with different bend angles and dipole moments. The alkyl chains attached to all four compounds are identical and may be expected to adopt a very similar distribution of conformations at the same reduced temperature at which the measurements of the flexoelectric coefficients are made. The compounds have very similar lengths but different shapes with variations in the bend angle,  $\Theta$ , between 0.2 and 0.35. Compound **1** is almost cigar-shaped and the bend angle of the banana-shaped molecule increases in the order **3**, **2**, and **4**. All four molecules have a similar length. Compound **2** has a surprisingly large value of  $e/k$ , especially considering its relatively low dipole moment. Otherwise, the values of  $e/k$  are similar for E7 and ZLI-4792, suggesting that the quadrupolar flexoelectric effect in E7 plays a minor role in the doped mixtures. Figure 4 shows  $\Theta$  and  $\mu$  as a function of  $e/k$  in ZLI-4792. Interestingly, more linear molecules give a larger flexoelectric effect and there is no correlation between the flexoelectric coefficients and the dipole moment of the dopants. Compound **4** has the most bent structure and

(24) Takahashi, T.; Hashidate, S.; Nishijou, H.; Usui, M.; Kimura, M.; Akahane, T. *Jpn. J. Appl. Phys.* **1998**, *32*, 1865.

(25) Madhusudana, N. V.; Durand, G. *J. Phys. Lett.* **1985**, *46*, L195.

(26) Warrior, S. R.; Madhusudana, N. V. *J. Phys. II France* **1997**, *7*, 1789.

(27) Blinov, L. M.; Barnik, M. I.; Ohoka, H.; Shtykov, N. M.; Yoshino, K. *Eur. Phys. J. E* **2001**, *4*, 183.

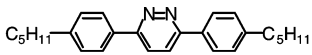
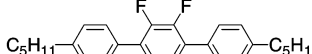
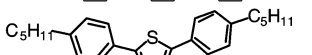
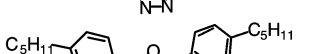
(28) Mazzulla, A.; Ciuchi, F.; Sambles, J. R. *Phys. Rev. E* **2001**, *64*, 21708.

(29) Jewell, S. A.; Sambles, J. R. *J. Appl. Phys.* **2002**, *92*, 19.

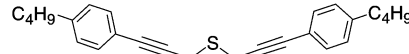
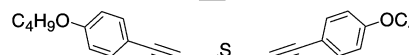
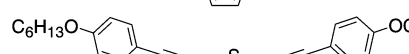
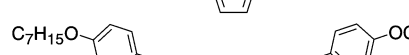
(30) *Molecular Modelling Software*, Molecular Simulations Inc., 230/250 The Quorum, Barnwell Road, Cambridge CB5 8RE, U.K. (<http://www.msi.com>).

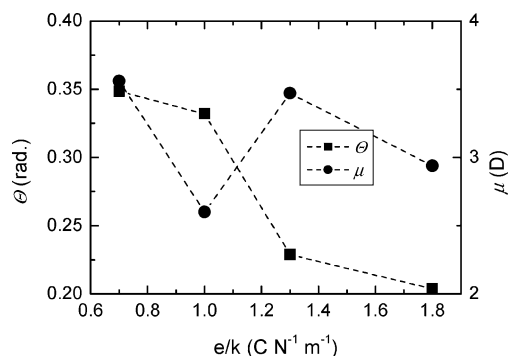
(31) Leadbetter, A. J.; Richardson, R. M.; Collings, C. N. *J. Phys.* **1975**, *36*, 37.

Table 1. Tabulated Results for Guest–Host Mixtures Containing Compounds 1–4 in E7 and ZLI-4792<sup>a</sup>

	$\Theta$ (rad)	$\mu_L$ (D)	$a$ (Å)	$e/k$ in E7 (C N <sup>-1</sup> m <sup>-1</sup> )	$e/k$ in ZLI-4792 (C N <sup>-1</sup> m <sup>-1</sup> )
Pure host				0.9	0.6
<b>1</b> 	0.20	2.94 outward	26.7	1.7	1.8
<b>2</b> 	0.33	2.6 outward	24.8	2.2	1.0
<b>3</b> 	0.23	3.46 inward	22.7	1.4	1.3
<b>4</b> 	0.35	3.56 inward	21.8	0.5	0.7

<sup>a</sup> All results were obtained at 0.98 T<sub>N-I</sub>.Table 2. Tabulated Results for Guest–Host Mixtures Containing Compounds 5–8 in E7<sup>a</sup>

	Cr °C	N °C	I °C	$\Theta$ (rad)	$\mu_L$ (D)	$a$ (Å)	$e/k$ in E7 (C N <sup>-1</sup> m <sup>-1</sup> )
Pure host							0.9
<b>5</b> 	• 72	• 81	•	0.23	0.74	23.9	3.0
<b>6</b> 	• 95	• 168	•	0.25	3.14	27.7	3.0
<b>7</b> 	• 81	• 137	•	0.22	2.82	30.5	3.8
<b>8</b> 	• 79	• 126	•	0.14	2.08	33.6	3.4

<sup>a</sup> All results at 0.98 T<sub>N-I</sub>.Figure 4.  $\Theta$  and  $\mu$  are plotted as a function of  $e/k$  in ZLI-4792.

also induces the smallest change in the flexoelectric coefficients. This is consistent with the results above, which indicate that long, thin molecules exhibit the largest flexoelectric effect. However, both of these results disagree with expectations from dipolar theory.

A number of symmetric thiophenes (**5–8**) with systematic variations in the molecular properties were prepared. As Table 2 shows, compounds **5** and **6** differ only by the substitution of the butyl group in **5** for the butoxy group in **6**. This results in a large increase in the inward pointing dipole moment but  $e/k$  is the same for both compounds. The

latter result is surprising because the larger transverse dipole moment of the pure material octyloxy-cyanobiphenyl (8OCB) gives an  $e/k$  value 5 times higher than that of the alkyl homologue cyanobiphenyl (8CB).<sup>32</sup> Compounds **6–8** have alkoxy end groups of increasing length. Although there are no consistent systematic variations of  $e/k$  with molecular parameters, the dopant has a large effect on the flexoelectric coefficients, increasing  $e/k$  of the host by a factor between 3 and 4. The liquid crystal transition temperatures for the component thiophenes (**5–8**) are shown in Table 2.

Dimesogens with longitudinal dipoles have been shown to enhance the flexoelectric switching of chiral nematic liquid crystals.<sup>6,33,34</sup> They do not have a higher value of  $e/k$ , but reduce the dielectric coupling so that the helical structure necessary for device operation is retained for higher electric fields.<sup>6</sup> Dimesogens typically have a high viscosity so that devices using guest–host mixtures rather than pure compounds would have much faster switching times. The

(32) Luckhurst, G. R. Private communication. Aziz, N.; Ferrarini, A.; Grosse, M. C.; Kelly, S. M.; Jackson, D. J. B.; Luckhurst, G. R.; Schott, C. *Proceedings BLCS*, 016, 2005.

(33) Dozov, I.; Martinot-Lagarde, Ph.; Durand, G. *J. Phys. Lett.* **1983**, *44*, L-817.

(34) Blatch, A. E.; Coles, M. J.; Musgrave, B.; Coles, H. *J. Mol. Cryst. Liq. Cryst.* **2003**, *401*, 161.

Table 3. Tabulated Results for Mixtures Made from Compounds 9–13 in E7 at 0.98 T<sub>N-1</sub>

	m	n	Cr °C	SmC °C	N °C	I	$\Theta$ (rad)	$\mu_{\perp}$ (D)	<i>a</i> (Å)	<i>e/k</i> in E7 (C N <sup>-1</sup> m <sup>-1</sup> )	
<b>9</b>	3	7	•	84	(•	77)	•	0.75	2.57	28.5	1.7
<b>10</b>	3	10	•	106	•	120	•	0.35	1.89	34.5	3.0
<b>11</b>	3	11	•	92	•	97	•	0.51	2.16	32.5	0.6
<b>12</b>	3	12	•	108	•	113	•	0.31	2.50	33.8	3.4
<b>13</b>	5	10	•	97	•	99	•	0.12	2.45	41.1	4.7

dimesogenic approach allows the length of mesogens to be varied over a wide range. Dimesogens also show an odd–even effect in the spacer length which enhances variations in the bend angle of the compounds. Hence, dimesogens were chosen as model compounds for this work and data from this series are shown in Table 3. We study dimesogens with transverse rather than longitudinal dipoles. The odd–even effect in the liquid crystal transition temperature for the symmetrical dimers **10**–**12** is shown in Table 3. The melting and clearing points of compound **11** are lower (Cr–N = 92 °C; N–I = 97 °C) than those (Cr–N = 106 °C; N–I = 120 °C, and Cr–N = 108 °C; N–I = 113 °C, respectively) of compounds **10** and **12**, respectively. There is usually a direct correlation between the value of the nematic clearing point and the geometric ratio *a/b* for simple space-filling reasons dependent on molecular shape. Hence, the lower nematic clearing point of the homologue **11** with an odd number of methylene units (CH<sub>2</sub>) in the central aliphatic spacer is attributed to the lower length-to-breadth ratio, *a/b*, and consequently higher bend angle as shown, compared to that of the homologues **10** and **12** with an even number of methylene units (CH<sub>2</sub>) in the spacer group. Compound **9**, with a short (CH<sub>2</sub>)<sub>7</sub> spacer, has also a low clearing point and a monotropic liquid crystal phase. The addition of a small % of dopant has a remarkable effect on the flexoelectric coefficients: doping with 10 wt % of compound **13** increases *e/k* from 0.9 to 4.7 C N<sup>-1</sup> m<sup>-1</sup>.

The flexoelectric coefficients are also a property of dopant concentration. For example, *e/k* of compound **10** increases from 1 C N<sup>-1</sup> m<sup>-1</sup> at a dopant concentration of 5 wt % to a saturated value of 3.5 C N<sup>-1</sup> m<sup>-1</sup> above 25 wt %. Although the variation of *e/k* with molecular parameters is not completely consistent across the series, some trends can be identified. There is little correlation with dipole moment but *e/k* tends to decrease with increasing bend angle. As discussed in more detail below, this is exactly the opposite effect to that predicted from dipolar models of flexoelectricity.

Results from the heterocyclic three-ring compounds **1**–**4** and dimesogen series **9**–**13** suggest most clearly that *e/k* is correlated with the bend angle. Results from the three series suggest that there is no correlation with the transverse dipole moment of the compounds. It is not yet obvious whether the molecular length of the dopant influences flexoelectricity. We now attempt to identify any general trends by examining

the dependence of *e/k* of all guest–host mixtures in E7 on the dopant parameters  $\Theta$ ,  $\mu$ , and *a*. Figure 5a plots *e/k* versus  $\Theta$ . A different symbol is used for each of the three classes

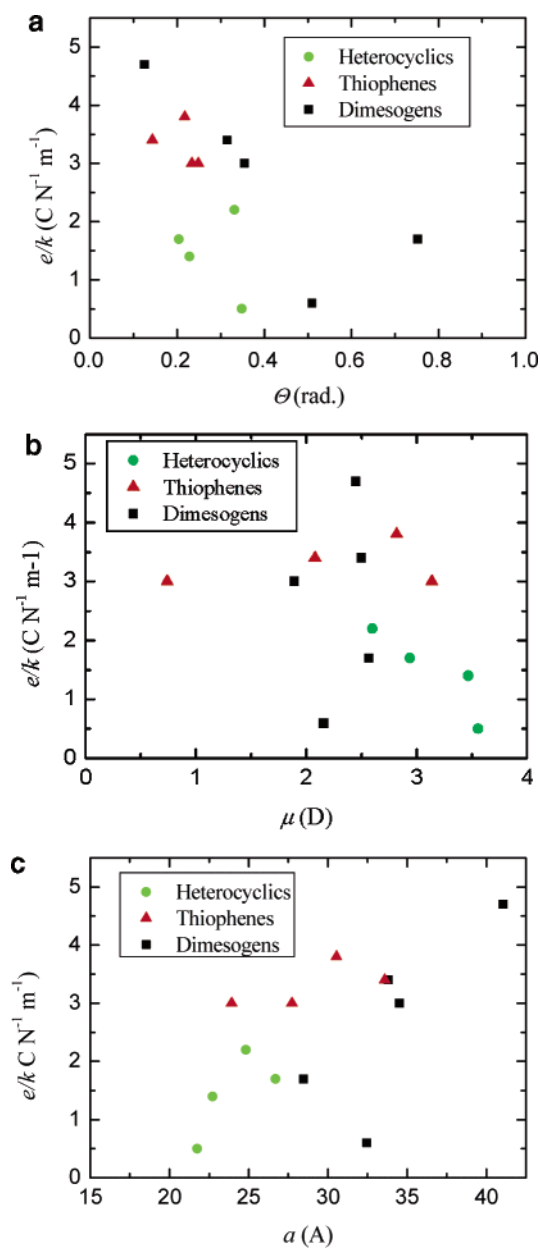


Figure 5. (a) *e/k* is plotted versus  $\Theta$ . (b) *e/k* is plotted versus  $\mu$ . (c) *e/k* is plotted versus *a*.

of compounds. Although there is some scatter from data, and the datum from compound **9** is anomalous, it is clear that  $e/k$  has an inverse relationship with  $\Theta$ ; i.e., the more curved the banana-shaped molecule, the *smaller* the flexoelectric effect. This appears to be in contradiction with the dipolar theories, which predict a linear increase of the flexoelectric coefficients with  $\Theta$ . The dipolar models also predict an increase in flexoelectricity with the lateral dipole moment of banana-shaped molecules. As Figure 5b shows, there is no correlation between  $e/k$  and  $\mu$ . Figure 5c shows a general increase of  $e/k$  with  $a$  particularly for the heterocyclic and dimesogenic series, although the scatter from the data is high. We must be careful not to reject dipolar coupling as the origin of the enhanced  $e/k$  for the guest–host mixtures.  $\Theta$  is defined as the bend angle for the energy-minimized configuration in the gaseous state. In the liquid crystal state different conformations may be preferred. Longer molecules are more easily deformed and the dimesogenic series is particularly flexible because of the aliphatic link group. The observed increase of  $e/k$  with molecular length may suggest a link with the flexibility of the molecule. The splay-bend deformation induced by the hybrid aligned nematic configuration may impose a more bent conformation on the dopants. Their shape imposes a polarization because of their transverse dipole moment. The more numerous dipoles of the host molecules will also couple to the shape and polarization polarity of the dopant so that

the magnitude of  $e/k$  is not correlated with the magnitude of the dipole moment of the dopant.

#### IV. Conclusions

We show that guest–host mixtures of nematic liquid crystals, where the dopant has a transverse dipole moment, provide a viable route to greatly enhancing the flexoelectric effect for bistable LCDs. This approach is particularly attractive for the synthetic chemist because there are less severe constraints on other important material parameters for displays, such as viscosity, elastic constants, and transition temperatures since the dopant is used in low concentrations. This work informs the future design of new materials for flexoelectric displays. We show that long molecules with small bend angles are particularly suitable as dopants. Dimesogens are an attractive class of dopant. Unlike those used for chiral flexo displays, we find that dimers without longitudinal moments greatly enhance the flexoelectric effect. Our results can be explained using dipolar theories but more work is required to establish the specific mechanism, whether dipolar, quadrupolar, or other, responsible for the large enhancement of the flexoelectric coefficients in the guest–host mixtures.

**Acknowledgment.** We thank Qinetiq and EPSRC for financial support. D. Coates is thanked for useful discussions.  
CM051682Y